Research Article

Pyrolysis Kinetic Modelling of Wheat Straw from the Pannonian Region

Ivan Pešenjanski, Biljana Miljković, and Marija Vićević

Faculty of Technical Sciences, University of Novi Sad, Trg Dositeja Obradovića 6, 21125 Novi Sad, Serbia

Correspondence should be addressed to Ivan Pešenjanski; pesenjanskiivan@gmail.com

The pyrolysis/devolatilization is a basic step of thermochemical processes and requires fundamental characterization. In this paper, the kinetic model of pyrolysis is specified as a one-step global reaction. This type of reaction is used to describe the thermal degradation of wheat straw samples by measuring rates of mass loss of solid matter at a linear increase in temperature. The mentioned experiments were carried out using a derivatograph in an open-air environment. The influence of different factors was investigated, such as particle size, humidity levels, and the heating rate in the kinetics of devolatilization. As the measured values of mass loss and temperature functions transform in Arrhenius coordinates, the results are shown in the form of saddle curves. Such characteristics cannot be approximated with one equation in the form of Arrhenius law. For use in numerical applications, transformed functions can be approximated by linear regression for three separate intervals. Analysis of measurement resulting in granulation and moisture content variations shows that these factors have no significant influence. Tests of heating rate variations confirm the significance of this impact, especially in warmer regions. The influence of this factor should be more precisely investigated as a general variable, which should be the topic of further experiments.

1. Introduction

The widespread availability of biomass, which is renewable and has no impact on global warming, has motivated extensive research in the past decade regarding the industrial development of thermochemical conversion plants. Pyrolysis, an important step in all thermochemical processes, is a technology that has the potential to reduce dependence on fossil resources by providing alternative fuels or useful chemicals. Also, pyrolysis will be essential in new technologies such as low temperature carbonization and chemical production from solid fuels. Understanding pyrolysis kinetics is important for the effective design and operation of conversion units.

Extensive reviews based on a number of papers done by Antal Jr. and Varhegyi [1] and Di Blasi [2] show that the pyrolysis of biomass involves a complex series of reactions. Consequently, changes in the experimental heating conditions or sample composition and preparation may affect not only the rate of reaction but also the actual course of the reactions. Most of these observations which are made from reported publications have been mainly focused on woody material and, in a few cases, on agricultural residues. Cereal straws are the predominant biomass in Pannonian agricultural areas, where wood waste is much less available.

Early researches of wheat straw combustion [3–5] have pointed out the fact that gaseous products comprise 70–85% of total pyrolytic reactions products. Temperatures at which they emerge are also notably low (200–450°C) [4, 5]. The most intensive reactions are noticed at around 300°C, so it is very likely that the largest part of gaseous and solid products of reaction under these conditions do not react with considerable acceleration of oxidation at first contact with the oxidant, which could be characterized as ignition. Reference [6] has confirmed the conclusion of Shafizadeh [3] that the thermal decomposition of cellulose over a wide range of mass loss is essentially the same in both air and nitrogen. At the beginning of the decomposition oxygen interacts only with surface cellulose, resulting in only ~3% of mass loss. This gives

a reliable basis for the assumption that pyrolysis prevails in regions where chemical kinetics restricts the overall rate of the combustion process.

However, variability of ash composition and ash content in straw (1–15%) seems to have a strong influence on both the pyrolytic characteristics and the product distribution (catalytic effect of the ashes) [2, 7, 8]. This means that results obtained from the analysis of single components cannot be directly applied to wheat straw because of chemical and physical alterations introduced in the separation procedure, the impossibility to reproduce component interactions, and the presence of ash [2, 9]. Ash constituents, especially potassium (K), sodium (Na), and calcium (Ca), act as catalysts for the decomposition process. As chlorine (Cl) and potassium in biomass are water soluble, they can, for the most part, be removed through leaching, thus mitigating their impact on the high-temperature conversion devices. In reality, water or mild acid washing also introduce significant modifications in biomass decomposition characteristics [9, 10].

Quantitative differences between characteristics are caused by several factors which, in addition to the biomass species, include, even for the same sample, the geographical origin, the age, or the specific part of the plant [10, 11]. All these observations justify the need for a detailed investigation of every specified case.

The aims of this research were to investigate the pyrolytic behavior of wheat straw from Vojvodina, to check the influence of experimental conditions on the kinetic parameters, and to provide kinetic information for the evaluation of the processing of these materials.

2. Mathematical Model of Pyrolytic Processes

In reality, thermal decomposition in wheat straw involves numerous physical impacts with complex chemical reactions and ends up with a large number of intermediates and end products. On the other hand, pyrolytic models are created on the basis of visible and measurable reflections. However, our understanding, through experimentation, of the basic processes occurring during the combustion/pyrolytic process is very limited and still questionable [12, 13].

A further general approach is considered in this paper: virgin biomass as the raw material and with gas/volatiles and solid char/coke yield as the end products (one-step global model [13]).

Diffusion effects in TGA tests are particularly important as the pyrolysis process involves the transport of reactant and heat from the external bulk gas phase to the internal particle surface, where the chemical reactions take place. Hence pyrolytic models can be subdivided, depending on intensity of the diffusion effect influence on microparticle models and macroparticle models [14].

Pyrolysis of microparticles includes thermal decomposition of the virgin matter in samples of sufficiently small dimensions, so that the effects of diffusion become negligible, and the intensity of pyrolysis is confined and controlled with kinetics (kinetic region of reaction). This fact enables the phenomenology of kinetics to be investigated on microparticles.

Critical particle dimensions that are set for kinetic control generally range from about 100 to 1000 μm [14] and it has been noticed that they grow with the temperature of pyrolysis [11, 14]. Particles larger than the critical one are characterized by greater diffusional effects which can intensively influence the development of pyrolysis through internal and external temperature gradients, heat inertia, and temperature variations due to the occurrence of exothermic and endothermic reactions, which should be avoided in this work. References [14–16] give a more detailed model that is able to describe the kinetics, the heat transfer, and the mass fluxes that take place during biomass combustion/pyrolysis of samples with macroparticles (more near to real technical objects).

2.1. Kinetic Modelling. Abstracting the concrete content of all processes with the uniform pyrolytic reaction (unified lumped approach, one-step global model), kinetics of the total reaction can be expressed through Arrhenius monomolecular equation of the first order. As the volatiles in this simplified model represent the "subject of motion," it is natural that the law of change in mass, hypothesis, is set in such a way so that the rate of volatile extraction is proportional to the quantity of remaining volatiles in the fuel. Based on that, the mathematical form of pyrolysis reaction rate can be expressed by the following equation:

$$\rho \frac{dm_v}{d\tau} = (1 - m_v)\, k \exp\left\{ -\frac{E}{(\Re T)} \right\}. \tag{1}$$

In the laboratory conditions measuring the remaining mass of the solid residue (char) ($m_v = 1 - m_v$) can be done more easily. As needed, (1) may be rearranged to

$$-\frac{dm_c/d\tau}{m_c} = \frac{k}{\rho} \exp\left\{ -\frac{E}{(\Re T)} \right\}. \tag{2}$$

In the presented form (2) has the dimension of s^{-1}, so that the preexponential multiplier k has the dimension of kg/(m^{3}s) (mass flux per volume). The rate of the heterogeneous reaction (sometimes called char reactivity) is expressed per unit of area of reacting material, so for the purpose of comparison with the mass transfer coefficient, as generally is with the use of the complex resistance method, this value is necessary to correct with the multiplier of the ratio of volume and area of combustible matter.

With finding the logarithm of (2) and introduction of Arrhenius variables of temperature and mass loss rate retrospectively,

$$X = \frac{1000}{T},$$
$$Y = \ln\left\{ -\frac{dm_c/d\tau}{m_c} \right\}, \tag{3}$$

(2) in coordinates of Arrhenius for k = const. gets first-order polynomial form

$$Y = a_0 + a_1 X, \tag{4}$$

which is convenient to fit with experimental data. In (4) polynomial coefficients are

$$a_0 = \ln \frac{k}{\rho},$$

$$a_1 = -\frac{E}{\mathfrak{R}}. \tag{5}$$

It should be mentioned that the differential equation (2), despite its simple form, does not have an analytical solution.

For the reason that organic substances are preexponential multiplier and activation energy dependent on temperature, that is, $k = k(T)$ and $E = E(T)$, therefore based on that, they have to be calculated in nonlinear form, for example, with n degree polynomial:

$$Y = \sum_i a_i X^i, \quad i = 0, 1, 2, \ldots, n. \tag{6}$$

In real coordinates, (6) returns to the following:

$$-\frac{dm_c/d\tau}{m_c} = \prod_i \exp \left\{ a_i \left(\frac{1}{T} \right)^i \right\}, \quad i = 0, 1, 2, \ldots, n. \tag{7}$$

Both of the models (4) and (6) may be used for the standalone pyrolysis applications as well as a submodel in a CFD code with more complex models [17, 18]. A computer program using C++ is required to perform written calculations.

2.2. Influence of Mass Diffusion through the Gas Phase. In 1924, Nusselt [19] proved through theoretical analysis that smaller particles "burn faster" due to decreased diffusion resistance. The question is how small should the investigated particle size be in which diffusion will occur much faster than the kinetics of pyrolysis?

Knowing that the Nusselt number is a dimensionless temperature gradient integrated over the surface and that the Sherwood number is a dimensionless concentration gradient integrated over the surface, correlations for binary mass transfer coefficients at low mass transfer rates can be obtained the same way and directly from their heat transfer analogs simply by a change of notation (Nu by Sh and Pr by Sc) [20].

Bird et al. (after Froessling, 1938) [20] gave a correlation for predicting the heat transfer to or from a sphere with constant surface temperature by the following empiricism:

$$\text{Nu} = 2 + 0{,}552\text{Re}^{1/2}\text{Pr}^{1/2} \tag{8}$$

(which also takes into account current adjustments by the constants in the second summands at 0,60). Equation (8) is also valid for small net heat/mass transfer rates. If there are stagnant conditions (Re = 0), (8) develops to "Newton's law of cooling":

$$\text{Nu} = \text{Sh} = 2 \tag{9}$$

(this well-known result also provides the limiting value of Nu for heat transfer from spheres at low Reynolds and Grashof numbers). While the Sherwood number is

$$\text{Sh} = k_m \cdot \frac{d}{D}, \tag{10}$$

binary diffusion coefficient D can be determined from the Schmidt number

$$\text{Sc} = \frac{\nu}{D}. \tag{11}$$

Solving (9), (10), and (11), the mean mass transfer coefficient is obtained

$$k_m = 2 \cdot \frac{\nu}{(d \cdot \text{Sc})}. \tag{12}$$

The Schmidt number for gases does not vary greatly with temperature; it does, however, vary significantly with mixture ratio. The Schmidt number is for a dilute binary mixture of volatile gases (CO_2, CO, H_2, and CH_4) typically present in air [21]; Sc = 0,6–1,0 ≈ 0,8. The viscosity of a volatile mixture is not simply a function of the composition; it varies with temperature. For dilute binary mixtures of typical flue gases with air in a temperature range of 200°C–400°C the viscosity of a volatile-air mixture is $\nu = (32{,}8\text{–}60{,}4) \cdot 10^{-6}$, m^2/s.

When these values are used in (12) we get the hyperbolic dependence of mass transfer coefficient from particle size. For typical wall thickness of the straw $d \sim 0{,}5$ mm, the mean mass transfer coefficient is found to be

$$k_m = (0{,}14\text{–}0{,}25), \ \text{m} \cdot \text{s}^{-1}. \tag{13}$$

The requirement that during the experiment mass diffusion does not inhibit the kinetics of pyrolysis is that mass diffusion must take place much faster than the sample mass change occurring through chemical kinetics:

$$\frac{dm_c/d\tau}{m_c} \cdot \frac{d}{6} \ll k_m, \tag{14}$$

where the correction factor $d/6$ is the ratio of particles volume and surface:

$$\frac{d}{6} = \frac{V}{F}. \tag{15}$$

3. Methodology: Setup and Procedure

3.1. Samples. Wheat straw samples were collected for research from an agricultural area near Novi Sad (Serbia) in two-year intervals. The wheat type is "Novosadska rana 5" which is commonly sown in Vojvodina (Serbia). The wheat was treated with standard agrotechnical measures. A simple random sampling plan was used in order to get samples immediately after harvest from the collecting warehouse during the dry weather, not exposing the straws to bad climate influences. The collected stalks were air-dried naturally in a dry store room in ambient condition. Its proximate and ultimate analysis are given in Table 1, and its ash melting behavior is given in Table 2.

In order to keep the representation of the stalk solid part content while simultaneously paying attention to the proportion and to achieve the granulation of 0,3–0,4 mm, samples of straw were crushed and ground in a rotary mill and sieved to provide a feed sample in the size range of about 0,35 mm. During the sample formation of finely grinded straw (<0,1 mm) the mill was used with high angular speed. For tests with entire pieces of straws, they are cut to lengths of 15 to 20 mm.

TABLE 1: Proximate and ultimate analysis of wheat straw [22].

Parameter	Unit	Method	Amount (ad[1])	Amount (daf[2])
Moisture	mass-%	DIN EN 14774-1	3,7	—
Ash (550°C)	mass-%	DIN EN 14775	5,2	—
Volatile matter incl. moisture	mass-%	DIN CEN/TS 15148	79.0	82,3
Fixed carbon	mass-%	DIN 51734	16,2	17,7
Carbon	mass-%	DIN EN 15104	44,8	48.9
Hydrogen	mass-%	DIN EN 15104	5,51	6,02
Nitrogen	mass-%	DIN EN 15104	0,65	0,72
Oxygen	mass-%	DIN CEN/TS 15296	40,2	43,9
Sulphur	mass-%	DIN EN 15289	0,053	0,058
Chlorine	mass-%	DIN EN 15289	0,31	0,34
Fluorine	mass-%	DIN EN 15289	<0,005	<0,005
Phosphorus	mass-%	DIN CEN/TS 15410	0,053	0,058
Potassium	mg/kg	DIN CEN/TS 15410	6700	7400
Gross heating value	MJ/kg	DIN EN 14918	17,7	18,4
Net heating value	MJ/kg	DIN EN 14918	16,4	17,2

ad[1]: result calculation to "air dry" state.
daf[2]: result calculation to "dry and ash free" state; calculation base is the ash amount at 815°C.

TABLE 2: Ash melting behavior (ash fusion temperatures) (oxidizing atmosphere) [22].

Parameter	Unit	Method	Amount
Deformation temperature	°C	DIN CEN/TS 15370	1156
Hemisphere temperature	°C	DIN CEN/TS 15370	1225
Flow temperature	°C	DIN CEN/TS 15370	1251

3.2. Experimental Apparatus and Procedures. The experimental work was carried out using the derivatograph MOM Budapest, type 3427. Sketch map of TG heating vessel and laboratory device are shown in Figure 1.

Thermal gravimetric analysis (TGA) provides the characteristics of samples mass changes under the influence of temperature changes during the last time at certain programmed temperature changes. Differential thermal analysis (DTA) measures the temperature difference between the analyzed sample and reference material at a sample temperature. TG curves of samples reflect the relationship between changes in the sample mass, temperature, and ambient gas in the heating vessel. Reference matter is formed of Al_2O_3 (an inert material). Therefore, thermogravimetric curves are measured for dynamic conditions [2] (ramp heating, inear temperature-time relationships). The DTA can also measure the temperature difference between the sample pans.

The sample pan size in all experiments was 200 mg. The temperatures of the thermobalance furnace and sample were measured by means of two Pt-PtRh-type thermocouples, located on the furnace wall and beneath the sample holder, respectively, as seen in Figure 1. The difference between furnace temperature and that of the sample was in the range of a few degrees in all the experiments. The detailed description of the experimental setup is provided in [11].

However, a brief summary of the setup is as follows: a small sample of starting material is weighed and spread evenly in a sample cup; the cup is then placed on the balance sample holder; the startup protocol is initiated; and finally, the sample was heated at a constant rate of heating to the desired final temperature.

Hypothesis set with (1) and (2) explicitly recognizes two variables of the process: straw sample temperature (T, °C) and sample heating rate ($dT/d\tau$, °C·s^{-1}).

Temperature is the "general variable" of the process (fundamental factor) and it varies between 160°C and 500°C (linear gradient against time) with temperature readings at intervals by 10°C (35 levels). Three readings were performed with each step, for the mass amount and for the mass rate, which gives nine values of the dependent variable (mass loss rate) for each independent variable (temperature). $9 \times 35 = 315$ readings must be done in one examination.

Heating rate ($dT/d\tau$, °C·s^{-1}), particle size (granulation) (d, mm), and sample moisture (W, %) are so called latent variables. Operating gradients of temperature are approved according to the possibilities of available devices (2,5; 5, 10, and 25°C·min^{-1}).

Based on the above theoretical considerations we come to the general conclusion that granulation size does not affect the kinetics in small samples (100 to 1000 μm). Not to mention the drying of small samples at a slow heating rate is carried out faster than it takes for the temperature to reach the value to start pyrolytic reactions. For these reasons, in order to evaluate the importance of effect size and moisture content of samples, only the impact of extreme and common values was examined.

TABLE 3: Experimental map.

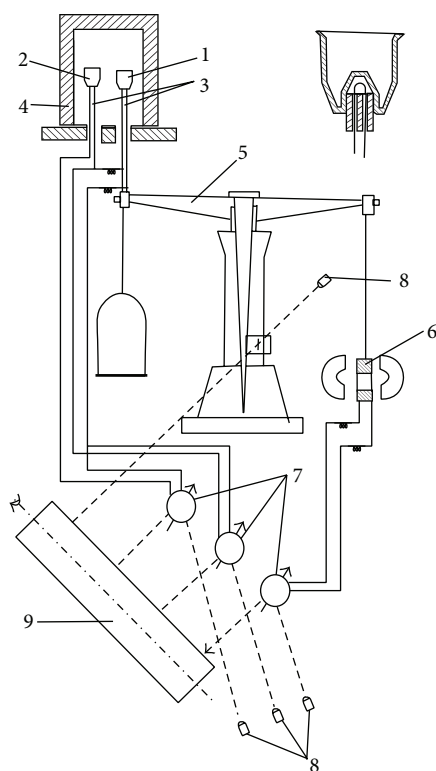| Label of experiment	Variable	Granulation size mm	Moisture %	Heating rate $dT/d\tau$, ˚C·s^{-1}
I	Granulation	**15–20**	Air-dried	5
II	**Granulation**	**0,3–0,4**	**Air-dried**	**5**
III	Granulation	**<0,1**	Air-dried	5
IV	Moisture	0,3–0,4	**~50%**	5
V	Moisture	0,3–0,4	**~20%**	5
VI	Moisture	0,3–0,4	**Dried**	5
VII	Heating rate	0,3–0,4	Air-dried	**2,5**
VIII	Heating rate	0,3–0,4	Air-dried	**10**
IX	Heating rate	0,3–0,4	Air-dried	**25**

FIGURE 1: Sketch map of TG heating vessel and laboratory device MOM Budapest, type 3427. 1: cup with sample measured; 2: cup with reference material; 3: thermocouples; 4: heating vessel; 5: analytical balance; 6: an induction assembly; 7: galvanometers; 8: light source; 9: photo sensitive recording.

The final map of experiments is shown in Table 3. A total of nine groups of experiments are planned.

As shown in Table 3, the first group of experiments (labeled as I, II, and III) are centered on studying the influence of variations in the size of granulation in the kinetics of mass loss. The second group of experiments (labeled as IV, V, and VI) is planned to investigate the effects of variations of moisture, and the third group (labeled as VII, VIII, and IX) is to examine the effect of variations. Since the results of all the experiments are compared to the experiment marked with II, this will be called the reference experiment.

4. Results and Discussion

4.1. Experimental Results. The experiments were replicated three times to determine their reproducibility, which was found to be good. More repetitions were carried out in case any variability was observed. With the entire set of experiments several thousand results were obtained (315 per experiment) which are impractical for displaying, even on the charts. The main experimental parameters obtained are shown in Table 4.

As shown in Table 4, the fastest reaction rate (peak) was observed in experiment IX, with the value of 23%·min^{-1}, which was obtained at 280˚C, and a heating rate of ~40˚C·min^{-1} and at 46% of primary sample mass. For comparison with the mean mass transfer coefficient in (12), the typical wall thickness of the straw $d \sim 0,5$ mm is calculated by Arrhenius term:

$$\frac{dm_c/d\tau}{m_c} \cdot \frac{d}{6} = \frac{23,0}{60 \cdot 46} \cdot \frac{0,5 \cdot 10^{-3}}{6}$$
$$= 0,69 \cdot 10^{-6} \, \text{m} \cdot \text{s}^{-1}. \tag{16}$$

Comparing the calculated value from (16) with the mean mass transfer coefficient (13) is obtained:

$$0,69 \cdot 10^{-6} \ll 0,14, \ \text{m} \cdot \text{s}^{-1}, \tag{17}$$

which means that the operating conditions are too slow to affect the kinetic parameters.

4.2. Reference Experiment. Five experiments were done in conditions labeled as II with a heating rate of 5˚C·min^{-1}, granulation of average thickness of the straw wall piece (approx. 0,35 mm), and hygroscopic moisture, from which two were completely identical (II and II-A), while with the

TABLE 4: Realized main parameters of the experiments.

| Label of experiment	Particle size mm	Moisture/char %/%	Heating rate, ˚C·min⁻¹ Temperature range, ˚C			Temperature at peak ˚C	Reaction rates peak %·min⁻¹
			200–300	300–400	400–500		
I	15–20	7,5/2,0	6,5	5,6	5,2	250	4,20
II	~0,35	8,0/3,5	7,3	5,3	5,3	260	5,30
II-A	~0,35	8,0/3,5	7,3	7,3	5,3	270	7,50
II-B	~0,35	9,1/8,9	8,6	5,0	3,9	270	10,00
II-C	~0,35	9,0/9,0	9,5	5,0	4,1	280	7,14
II-D	~0,35	7,5/3,5	6,8	5,2	5,1	260	7,69
III	<0,1	7,0/3,0	6,9	5,2	5,2	270	5,10
IV	~0,35	59,5/0,5	6,2	5,6	4,9	280	12,50
V	~0,35	26,5/0,5	6,5	5,4	5,5	270	4,22
VI	~0,35	4,0/6,0	6,6	5,6	5,4	270	8,27
VII	~0,35	8,0/2,8	3,4	3,0	2,7	260	2,04
VIII	~0,35	7,0/3,5	18,7	13,0	13,0	270	11,10
IX	~0,35	8,5/5,0	50,0	41,7	23,2	280	23,00

(a)

(b)
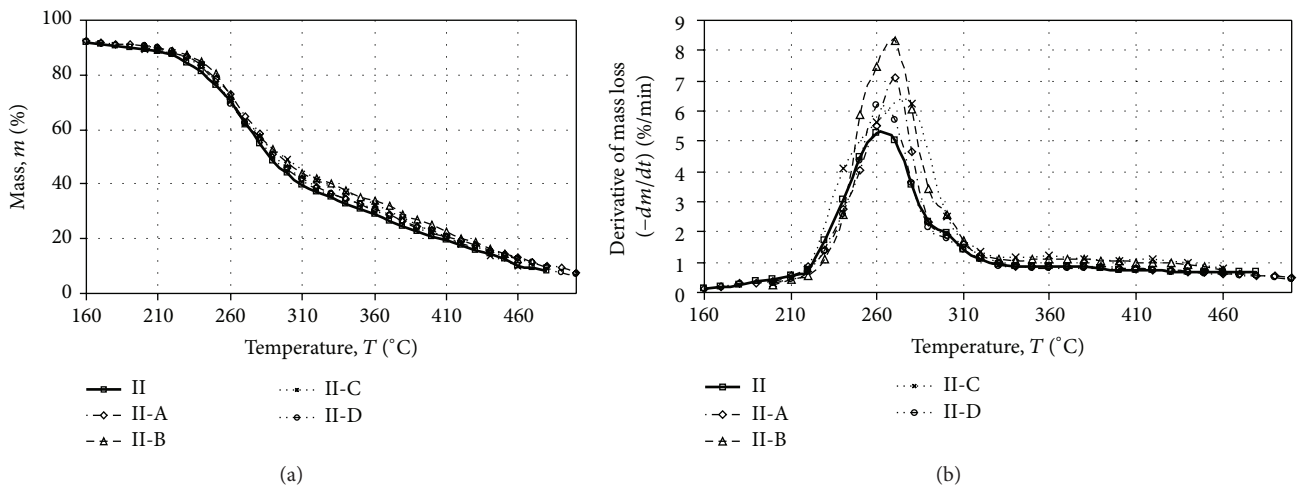
FIGURE 2: (a) TGA profile of wheat straw at experiments II; (b) DTG curves of experiments II.

others there were also small variations of humidity present (7,5–9,1%) and from the solid remain (3,5–9,0%).

Experiment II-C was carried out with a temperature range from 20 to 1000˚C in order to estimate the carbon content in the solid residue at 500˚C. As expected, the difference between the mass of solid residue was not significant after the completion of the reaction at 500 and 1000˚C.

The thermogravimetric weight/mass loss data (TGA) as a function of temperature are shown in Figure 2(a) and the derivatives of mass loss during pyrolysis (DTG) in Figure 2(b).

Actual readings of straw sample masses in function of temperature have no changes in the interval from 100 to 160˚C (inflection point); this is a result of the drying process during which pyrolysis has not yet started. On the figures presented in this work, only the temperature interval significant for pyrolysis is shown (>160˚C). No mass change appears at this temperature gradient higher than 450˚C, which points to the fact that up to this temperature all solid matter have already finished with pyrolytic reactions. The middle part of the curves is characterized by the intensive process of volatile extraction, which results in a steeper curve of mass change in the temperature interval from 230 to 280˚C. In Figure 2(b) (DTG) this phenomenon is manifested with a jump (peak) in function of mass loss rate in that interval. It is also important to notice that at this temperature interval only 50% of active sample mass reacts. In the region of higher temperatures it comes to a gradual slowing down of reactions, which is reflected in Figure 2(a) with an approximately constant slope of mass functions and in Figure 2(b) with a constant velocity of mass loss until the reaction ends.

As the measured values of mass loss/temperature functions transform in Arrhenius coordinates, the results are

TABLE 5: Kinetic parameters of wheat straw for the reference set.

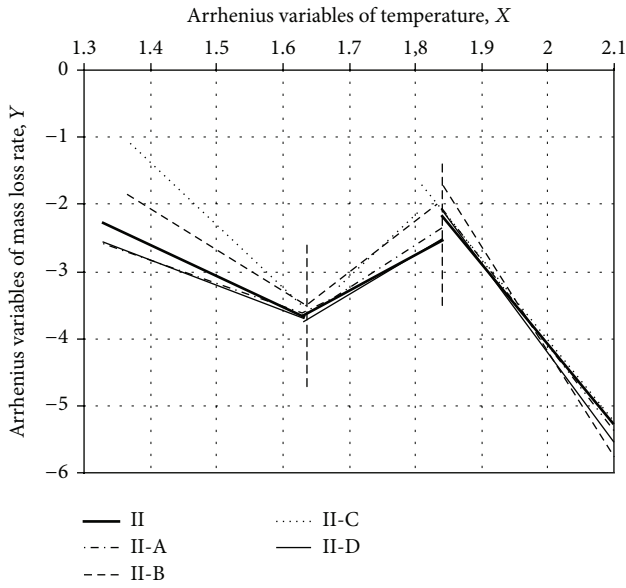| Experiment label	Region 1 $T < 270°C$		Region 2 $T = 270 \div 340°C$		Region 3 $T > 340°C$	
	k/ρ, 1/s	E, kJ/mol	k/ρ, 1/s	E, kJ/mol	k/ρ, 1/s	E, kJ/mol
II	$7,11 \times 10^6$	99,6	$79,0 \times 10^{-9}$	−43,9	0,85	38,8
II-A	$25,9 \times 10^6$	105	$10,5 \times 10^{-9}$	−53,9	0,113	28,3
II-B	9397×10^6	130	$2,24 \times 10^{-9}$	−62,6	12,79	50,5
II-C	$13,0 \times 10^6$	102	$0,09 \times 10^{-9}$	−78,1	1412	75,8
II-D	100×10^6	111	$25,0 \times 10^{-9}$	−49,2	0,183	31,1
Arithmetic mean	$74,3 \times 10^6$	109	$5,25 \times 10^{-9}$	−57,5	3,04	44,9

FIGURE 3: TGA of experiments around referent ones in Arrhenius coordinates.

shown in the form of saddle curves. Such characteristics cannot be approximated with an equation in the form of Arrhenius law. For use in CFD and similar numerical applications transformed functions can be approximated by linear regression in three separate intervals. The same approximations with polynomial regressions of the sixth degree for all experiments were also done in [11].

Numerical analysis is generally most easily developed through linear approximations while the different influences and trends can be more noticeably presented and examined. For that reason, linear approximations of five performed experiments are given in Figure 3(a) around the reference experiment case in three temperature intervals in Arrhenius coordinates without entering all the readings. As shown, kinetics of thermal destruction of wheat straw as a whole depict a saddle curve with three emphasized characteristic segments referring to the following temperature intervals:

(i) region of low temperatures: up to 270°C, reg. (1),

(ii) transitional region: 270–340°C, reg. (2),

(iii) region of higher temperatures: >340°C, reg. (3).

The parameters determined by minimizing the sum of the squared differences between the experimental and predicted values for each stage are listed in Table 5.

Coefficient of determination R_p^2 according to calculated data also shows a high degree of concordance between results of linear regression and readings:

$$R_p^2 = 0,83 \div 0,99. \tag{18}$$

While examining data on apparent energy of activation (E) it can be noticed that, as a rule, temperatures in these regions vary between 100 and 111 kJ/mol (also 130 kJ/mol), which in principle is not a great deviation. Differences are noticed, however, when the values of the constant a_0 are compared which determine the preexponential factor k/ρ. On the other hand, in regions of high temperatures a clear trend of decrease in activation energy value is found in an increase of heating rate from 102 kJ/mol to 10,9 kJ/mol (10 times). The preexponential multiplier in the first region varies in the interval within $0,19–32,4 \cdot 10^6$ s^{-1}; however in the third region variations of this multiplier reach far more drastic proportions from 0,005 s^{-1} to 200000 s^{-1}! Transition in region 2 is characterized by negative values of the apparent activation energy, which is more a result of changes in the mass loss rate rather than being the impact of the exothermic reaction, although in this region these phenomena are indeed noticed.

4.3. Granulation, Moisture, and Heating Rate Influences.
Analysis of measurement results in granulation variations (Figure 4) showing that this factor has no significant influence on the postulated hypothesis. Critical dimensions of biomass granules/particle size, when physical effects start more considerably influencing the process of pyrolysis, are according to [4, 6] generally more than 1,0 mm. Taking into consideration that the thickness of the solid part of straw stalk is from 0,3 to 0,5 mm, the initial hypothesis is also experimentally confirmed in this work.

There are different opinions in the literature on the issue of influence. Stenseng et al. [23], for example, concludes, "only the results for pure cellulose are sensitive to the sample mass. The pyrolysis of wheat straw and washed wheat straw remains unaffected by an increase in sample mass." However, he gives no explanation for this conclusion.

On the other hand, Mani et al. [24] reviews the following: "increasing initial weight causes diffusion resistance for the

TABLE 6: Kinetic parameters of wheat straw at heating rate variation.

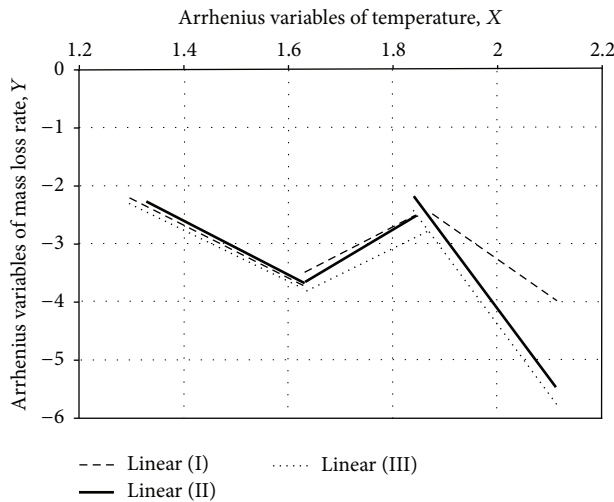| Experiment label	Region 1		Region 2		Region 3	
	k/ρ, 1/s	E, kJ/mol	k/ρ, 1/s	E, kJ/mol	k/ρ, 1/s	E, kJ/mol
VII	$0{,}19 \times 10^6$	87	$1{,}51 \times 10^{-6}$	−27	$0{,}20 \times 10^6$	102
II	$7{,}11 \times 10^6$	99,6	$79{,}0 \times 10^{-9}$	−43,9	0,86	38,8
VIII	$32{,}46 \times 10^6$	105	$34{,}4 \times 10^{-9}$	−52	0,03	13,6
IX	$1{,}21 \times 10^6$	89	$0{,}23 \times 10^{-6}$	−14	0,005	10,9

FIGURE 4: Influence of particle size on TGA (15 mm; 0,35 mm; <0,1 mm).

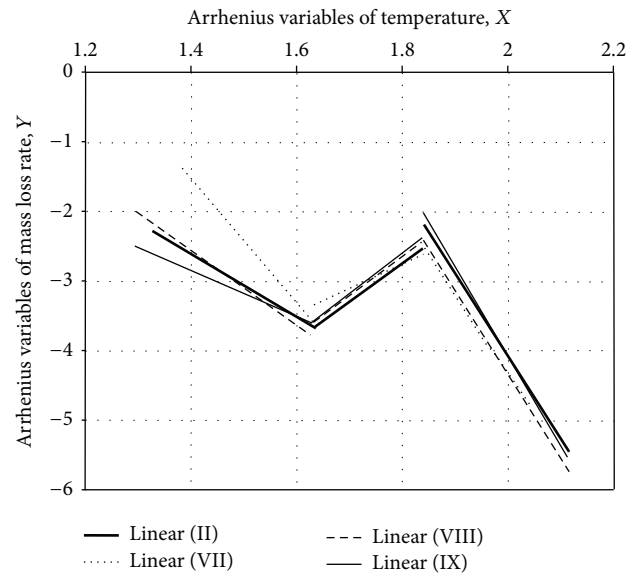FIGURE 5: Influence of moisture (4%; 8%; 26%; 60%).

devotilization," which is probably a basis to conclude that this effect does exist.

These opinions can be concluded as follows: securing enough small samples eliminates the effect of diffusion and thereby the influence of sample size and their initial weight/mass.

The character of TGA readings while treating moisture influence (Figure 5) is principally the same in all experiments. Similarly, when examining the diagrams it is possible to notice that the position of maximal mass change rate temperature also practically stays the same at all tests (270°C). Altogether it is possible to conclude that it is without reason that moisture content should also be treated as a general variable in experiments of pyrolysis which are determined in the setup of the work problem.

TGA readings of changes in Arrhenius coordinates when sample heating rate was varied (Figure 6) show that the general characteristics of process do not depend substantially on this variable. This relates especially to the range of lower temperatures where coefficients of slope change little with the change of experiment parameters. On the contrary, in the second half of reactions, that is, in regions of higher temperatures, significant variation is shown.

Calculated activation energies and preexponential factors which best fit the experimental data at heating rate variation are given in Table 6.

Mani et al. [24] also analyzed the effects of heating rate variations on wheat straw pyrolysis by thermogravimetry technique and obtained similar results as in this paper. The explanations of this phenomenon are, however, different. In [24] this is verbally explained on variability of the heat transfer effectiveness. For small particles and at quite a slow temperature gradient, this speculation without analytical or any other support seems unconvincing.

This paper stands on the views that it is a different chemical reaction that occur at different heating rate. In any case, this cannot be proved only by the results of a thermogravimetry technique. The conclusion should be that the impact of this factor should be explored with more complex procedures.

5. Conclusions

While investigating kinetic pyrolysis of wheat straw by thermal destruction in air, a form of characteristic is revealed which cannot be entirely qualitatively approximated with the unique reaction of the first order in the form of Arrhenius law.

Expressing the measured values as a function of Arrhenius variables, the saddle curve appears which represents three mutually different regions. Besides this, it is noticeable that the curves in regions of low and high temperatures (<270°C, >340°C) have the same trends, whereas in the transitional region the character of dependence is essentially
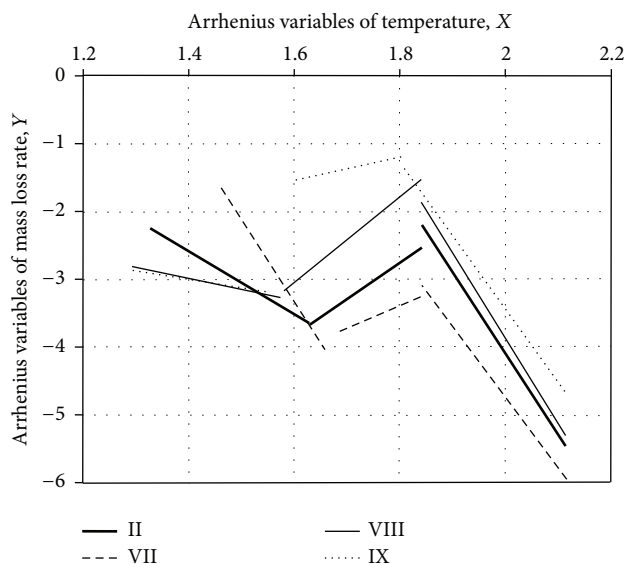
FIGURE 6: Influence of heating rate (2,5, 5, 10, and 25°C/min).

different. Statistical tests in particular regions show high significance to the law that is set by hypothesis (1).

There is no significant deviation from the reference experiment noticed when the granulation size of the wheat straw is varied, except in the case of piece material in regions of low temperatures (<270°C). Critical dimensions of biomass in general, when the physical limitations start more crucially to influence the resulting character of combustion, are, according to literature findings, from 0,1 to 1,0 mm. Taking into consideration that the thickness of the firm part of wheat straw stalks does not exceed 0,5 mm the stated hypothesis is also proven in this work.

As expected, moisture variations showed no sufficient significance. In the investigated range, drying processes are done in regions of lower temperature before the appearance of pyrolytic reactions which occur at higher temperatures (>160°C). Moisture content, however, does have an influence on the accurateness of measurement by shrinking the measuring range.

Variations in heating rate, however, do show significance in the second half of reactions, that is, in regions of higher temperatures where the second half of remaining mass reacts. On the contrary, the first half of reactions happens in the same way in all examined samples for discovered levels of heating rates, and statistical testing does not initiate a positive evaluation of significance for this influence in that region. The recommendation is that the influence of this factor should be more precisely investigated as a general variable, which should be the topic of further experiments.

Something noticed in all the investigations is that reactions start at temperatures of about 160°C, and temperatures of the highest mass loss rates were in the relatively narrow range of 260°C to 290°C when approximately 50% of the initial mass reacts. These parameters are significantly lower than the ones in similar works [3] which can be assumed to be a uniqueness of the sort of wheat under investigation.

Nomenclature

a_0, a_1: Polynomial coefficients
d: Particle size, granulation, equivalent spherical diameter of wheat straw grain particles, mm
D: Binary diffusion coefficient, m²/s
E: Activation energy, kJ/mol
k: Preexponential multiplier, kg/(m³s)
k/ρ: Preexponential factor, 1/s
k_m: Mean mass transfer coefficient, m/s
m: Mass fraction, kg, %
Nu: Nusselt's number
Pr: Prandtl's number
R, $\mathfrak{R}$: Universal gas constant, J/(mol K)
Re: Reynold's number
R_p^2: Coefficient of determination
Sc: Schmidt's number
Sh: Sherwood's number
T: Temperature, K
F: Particles surface area, mm²
V: Particles volume, mm³
W: Moisture of sample, %
X, Y: Arrhenius variables of temperature and mass loss rate retrospectively.

Greek Letters

β: Heating rate
ρ: Density, kg/m³
τ: Time, s
v: Viscosity, m²/s.

Subscripts

c: Char
i: Polynomial degree
v: Volatile.

Competing Interests

The authors declare that they have no competing interests.

References

[1] M. J. Antal Jr. and G. Varhegyi, "Cellulose pyrolysis kinetics: the current state of knowledge," *Industrial & Engineering Chemistry Research*, vol. 34, no. 3, pp. 703–717, 1995.

[2] C. Di Blasi, "Modeling chemical and physical processes of wood and biomass pyrolysis," *Progress in Energy and Combustion Science*, vol. 34, no. 1, pp. 47–90, 2008.

[3] F. Shafizadeh, "Pyrolysis and combustion of cellulosic materials," *Advances in Carbohydrate Chemistry*, vol. 23, pp. 419–474, 1968.

[4] F. Shafizadeh and A. G. W. Bradbury, "Thermal degradation of cellulose in air and nitrogen at low temperatures," *Journal of Applied Polymer Science*, vol. 23, no. 5, pp. 1431–1442, 1979.

[5] P. Perunović, I. Pešenjanski, and U. Timotić, "Biomass as a fuel," *Contemporary Agricultural Engineering*, vol. 9, no. 1-2, pp. 9–13, 1983.

[6] V. Mamleev, S. Bourbigot, and J. Yvon, "Kinetic analysis of the thermal decomposition of cellulose: the main step of mass loss," *Journal of Analytical and Applied Pyrolysis*, vol. 80, no. 1, pp. 151–165, 2007.

[7] K. Raveendran, A. Ganesh, and K. C. Khilar, "Influence of mineral matter on biomass pyrolysis characteristics," *Fuel*, vol. 74, no. 12, pp. 1812–1822, 1995.

[8] M. Lanzetta and C. Di Blasi, "Pyrolysis kinetics of wheat and corn straw," *Journal of Analytical and Applied Pyrolysis*, vol. 44, no. 2, pp. 181–192, 1998.

[9] A. Jensen, K. Dam-Johansen, M. A. Wójtowicz, and M. A. Serio, "TG-FTIR study of the influence of potassium chloride on wheat straw pyrolysis," *Energy and Fuels*, vol. 12, no. 5, pp. 929–938, 1998.

[10] G. Várhegyi, M. G. Grønli, and C. Di Blasi, "Effects of sample origin, extraction, and hot-water washing on the devolatilization kinetics of chestnut wood," *Industrial and Engineering Chemistry Research*, vol. 43, no. 10, pp. 2356–2367, 2004.

[11] I. Pešenjanski, *Kinetic reaction parameters of low-temperature wheat straw combustion [Ph.D. thesis]*, Faculty of Technical Science, Novi Sad, Serbia, 2002.

[12] G. Varhegyi, E. Jakab, and M. J. Antal Jr., "Is the broido-shafizadeh model for cellulose pyrolysis true?" *Energy and Fuels*, vol. 8, no. 6, pp. 1345–1352, 1994.

[13] N. Prakash and T. Karunanithi, "Kinetic modeling in biomass pyrolysis—a review," *Journal of Applied Sciences Research*, vol. 4, no. 12, pp. 1627–1636, 2008.

[14] R. S. Miller and J. Bellan, "A generalized biomass pyrolysis model based on superimposed cellulose, hemicellulose and lignin kinetics," *Combustion Science & Technology*, vol. 126, pp. 97–137, 1997.

[15] X. H. Liang and J. A. Kozinski, "Numerical modeling of combustion and pyrolysis of cellulosic biomass in thermogravimetric systems," *Fuel*, vol. 79, no. 12, pp. 1477–1486, 2000.

[16] A. A. Rostami, M. R. Hajaligol, and S. E. Wrenn, "A biomass pyrolysis sub-model for CFD applications," *Fuel*, vol. 83, no. 11-12, pp. 1519–1525, 2004.

[17] A. Galgano and C. Di Blasi, "Modeling the propagation of drying and decomposition fronts in wood," *Combustion and Flame*, vol. 139, no. 1-2, pp. 16–27, 2004.

[18] I. Pešenjanski, *Development of Facility for Energy Conversion of Baled Biomass for the Needs of Industry in Rural Valley Areas. Model of Macro Particle*, National Program for Energy Efficiency, Annual Report, Novi Sad, Serbia, 2005.

[19] W. Nusselt, *Der Verbrennungsvorgang in der Kohlenstaub-veuerung*, VDI, 1924.

[20] R. B. Bird, W. E. Stewart, and E. N. Lightfoot, *Transport Phenomena*, John Wiley & Sons, New York, NY, USA, 2002.

[21] W. M. Kays, *Convective Heat and Mass Transfer*, McGraw-Hill, New York, NY, USA, 1966.

[22] "Corn stover from Serbia," Test Report 1301674, SGS Institut Fresenius, Berlin, Germany, 2011.

[23] M. Stenseng, A. Jensen, and K. Dam-Johansen, "Investigation of biomass pyrolysis by thermogravimetric analysis and differential scanning calorimetry," *Journal of Analytical and Applied Pyrolysis*, vol. 58-59, pp. 765–780, 2001.

[24] T. Mani, P. Murugan, J. Abedi, and N. Mahinpey, "Pyrolysis of wheat straw in a thermogravimetric analyzer: effect of particle size and heating rate on devolatilization and estimation of global kinetics," *Chemical Engineering Research and Design*, vol. 88, no. 8, pp. 952–958, 2010.

Journal of
Engineering

The Scientific World Journal

International Journal of
Rotating
Machinery

Journal of
Sensors

International Journal of
Distributed
Sensor Networks

Advances in
Civil Engineering

Journal of
Control Science
and Engineering

Journal of
Robotics

Journal of
Electrical and Computer
Engineering

Advances in
OptoElectronics

VLSI Design

International Journal of
Navigation and
Observation

Modelling &
Simulation
in Engineering

International Journal of
Aerospace
Engineering

International Journal of
Chemical Engineering

International Journal of
Antennas and
Propagation

Active and Passive
Electronic Components

Shock and Vibration

Advances in
Acoustics and Vibration

Hindawi

Submit your manuscripts at
http://www.hindawi.com